Available online at www.sciencedirect.com
ScienceDirect
Journal of Power Sources 171 (2007) 155–168
JOURNAL OF POWER SOURCES
www.elsevier.com/locate/jpowsour

Experimental evaluation of the sensitivity to fuel utilization and air management on a 100 kW SOFC system

M. Santarelli [a,*], P. Leone [a], M. Calì [a], G. Orsello [b]

[a] *Dipartimento di Energetica, Politecnico di Torino, Corso Duca degli Abruzzi 24, 10129 Torino, Italy*
[b] *Gas Turbine Technologies, Corso Romania 661, 10156 Torino, Italy*

Received 14 September 2006; received in revised form 1 December 2006; accepted 11 December 2006
Available online 28 December 2006

Abstract

The tubular SOFC generator CHP-100, built by Siemens Power Generation (SPG) Stationary Fuel Cells (SFC), is running at the Gas Turbine Technologies (GTT) in Torino (Italy), in the framework of the EOS Project. The nominal load of the generator ensures a produced electric power of around 105 kW_e ac and around 60 kW_t of thermal power at 250 °C to be used for the custom tailored HVAC system.

Several experimental sessions have been scheduled on the generator; the aim is to characterize the operation through the analysis of some global performance index and the detailed control of the operation of the different bundles of the whole stack.

All the scheduled tests have been performed by applying the methodology of design of experiment; the main obtained results show the effect of the change of the analysed operating factors in terms of distribution of voltage and temperature over the stack.

Fuel consumption tests give information about the sensitivity of the voltage and temperature distribution along the single bundles.

On the other hand, since the generator is an air cooled system, the results of the tests on the air stoichs have been used to analyze the generator thermal management (temperature distribution and profiles) and its effect on the polarization.

The sensitivity analysis of the local voltage to the overall fuel consumption modifications can be used as a powerful procedure to deduce the local distribution of fuel utilization (FU) along the single bundles: in fact, through a model obtained by deriving the polarization curve respect to FU, it is possible to link the distribution of voltage sensitivities to FC to the distribution of the local FU.

The FU distribution will be shown as non-uniform, and this affects the local voltage and temperatures, causing a high warming effect in some rows of the generator. Therefore, a discussion around the effectiveness of the thermal regulation made by the air stoichs, in order to reduce the non-uniform distribution of temperature and the overheating (increasing therefore the voltage behavior along the generator) has been performed. It is demonstrated that the utilization of one air plenum is not effective in the thermal regulation of the whole generator, in particular in the reduction of the temperature gradients linked to the non-uniform fuel distribution.

Keywords: Tubular SOFC generator; Experimental session; Fuel consumption; Air stoichiometry; Local fuel utilization; Temperature distribution

1. Introduction

Gas Turbine Technologies (GTT) and Politecnico di Torino, both located in Torino (Italy), have installed a SOFC laboratory in order to analyze the operation, in cogenerative configuration, of the CHP-100 SOFC Field Unit built by Siemens Power Generation (SPG) Stationary Fuel Cells (SFC). The generator was commissioned on June 19, 2005, and to date has shown the record availability of 99.8%, showing more than 30,000 operating hours at this scale. The demonstration of this generator is the first phase of the EOS project (2004–2009), that has the following aims: (i) to establish a research group that, joining university and industry, will allow the growth of the scientific knowledge about SOFC technologies; (ii) to provide GTT with installation and operational know-how with SOFC; (iii) to extend life testing of SOFCs of varying pedigrees; (iv) to perform experimental and modeling activity to characterize the generator behavior. At present, approximately 100 kW_e of ac electrical energy are delivered to the grid, and 55 kW_t of thermal energy provides heating and cooling for the facility's buildings upon integration with a district HVAC. Politecnico di Torino has developed sev-

* Corresponding author. Tel.: +39 011 564 4489; fax: +39 011 564 4499.
E-mail addresses: massimo.santarelli@polito.it (M. Santarelli), pierluigi.leone@polito.it (P. Leone), michele.cali@polito.it (M. Calì), gianmichele.orsello@siemens.com (G. Orsello).

0378-7753/$ – see front matter © 2006 Elsevier B.V. All rights reserved.
doi:10.1016/j.jpowsour.2006.12.032

Nomenclature

BoP	balance of plant
CHP	cogeneration heat and power
$D_{i–j}$	fundamental binary diffusivity in the electrode ($cm^2\ s^{-1}$)
$D_{a(eff)}$	effective binary diffusivity in the anode layer ($cm^2\ s^{-1}$)
$D_{c(eff)}$	effective binary diffusivity in the cathode layer ($cm^2\ s^{-1}$)
E_0	open circuit voltage (V)
F	Faraday number ($C\ mol^{-1}$)
FC	fuel consumption (%)
FU	fuel utilization (%)
HC	high current
i_{as}	anode limiting current ($A\ cm^{-2}$)
i_{cs}	cathode limiting current ($A\ cm^{-2}$)
i_c	cell current density ($A\ cm^{-2}$)
I	generator current (A)
L	cell length (m)
LC	low current
p	cell pressure (Pa)
$p^a_{H_2}$	hydrogen pressure at the anode/electrolyte interface (Pa)
$p^b_{H_2}$	hydrogen pressure at the anode bulk (Pa)
$p^a_{O_2}$	oxygen pressure at the cathode/electrolyte interface (Pa)
$p^b_{O_2}$	oxygen pressure at the cathode bulk (Pa)
R	universal gas constant ($J\ mol^{-1}\ K^{-1}$)
SOFC	solid oxide fuel cell
t_a	thickness of the anode layer (cm)
t_c	thickness of the cathode layer (cm)
T	temperature (K)
T_{GEN}	setpoint temperature (K)
T_{air}	air pre-heating temperature (K)
V_c	cell terminal voltage (V)
V_{diff}	diffusion overpotential (V)
V_{nernst}	Nernst potential (V)
$\bar{V}_{Nernst}$	position averaged Nernst potential (V)
$\bar{V}_{Nernst,HC}$	average Nernst potential, high current approximation (V)
$\bar{V}_{Nernst,LC}$	average Nernst potential, low current approximation (V)
x	axial position along the tubular cell (m)
x_i	regressor variables
y_i	molar fraction of reactants at the electrodes' bulk
$y^0_{H_2}$	hydrogen molar fraction at fuel inlet condition
$y^0_{H_2O}$	water molar fraction at fuel inlet condition
Y_i	dependent variable

Greek letters

β_i	regression coefficient
ε	electrode porosity
$\eta_{act,a/c}$	activation overpotential at anode and cathode (V)
$\eta_{conc,a/c}$	concentration overpotential at anode and cathode (V)
η_{ohm}	ohmic overpotential (V)
λ_{air}	process air excess
τ	electrode tortuosity

eral activities, like the design of the SOFC primary generator thermal plant [1], the modeling of the generator and of the BoP [2–5], the safety design and analysis [6].

In particular, Politecnico has developed several experimental test and analysis of the experimental results. The experimental sessions have been designed in order to investigate the effect of four control factors at the nominal load operation: the fuel consumption FC, the air stoichs λ_{air}, the setpoint temperature T_{GEN}, and the air pre-heating temperature T_{air}. The methodology of the Design of Experiments has been used in the planning of the experimental session (factorial design) [7,8]. In [9] a model of the operation of the SOFC CHP 100 has been developed using a 0D approach and validated through a first session of experimental tests. In [10,11] the effect of the setpoint generator temperature and fuel utilization factors on several dependent variables (i.e. dc and ac electric power, recovered heat, electric and global efficiency, efficiency of the pre-reforming process) is analyzed in form of screening tests and the process responses are treated in form of response surface plots. In [12] the regression models have been used in constrained optimization procedures, to have an overview of the optimal operation points which maximize different objective functions (ac electric power, recovered heat, etc.).

The experimental tests showed that the most significant factors affecting the generator behavior are the fuel consumption FC and the air stoichs λ_{air}. In this paper results are presented concerning a deeper analysis of the sensitivity of voltage and temperature distribution to modification of fuel consumption and air stoichs. The aim is the deduction of the local distribution of fuel utilization (FU) along the single bundles, its drawbacks on temperature distribution (possible overheating), and a discussion concerning the temperature regulation through the air stoichs which outline some problems.

In [13] the sensitivity of the measured terminal voltage of a tubular solid oxide fuel cell to the fuel utilization is used to provide information about 'leaks' through the cell. In [14] an experimental analysis on a short stack is presented and the presence of localized overheating is addressed to low fuel availability on the anode side.

2. Experimental

2.1. Description of the plant

The CHP-100 kW_e SOFC Field Unit (SPG SFC) utilizes the commercial prototype air electrode supported cells (22 mm diameter, 150 cm active length, 834 cm^2 active area) and in-stack reformers. The generator is fed with natural gas from the grid.

Fig. 1. Picture of the SOFC CHP test site in GTT (Torino, Italy).

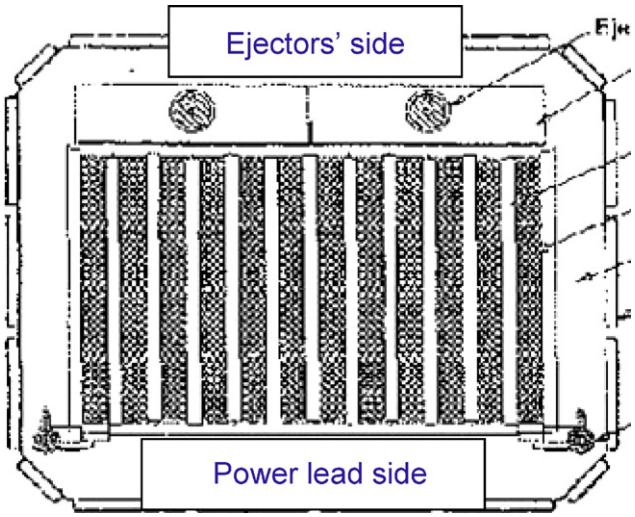

Fig. 2. Schematic of the stack arrangement.

In Fig. 1 the picture representing the CHP 100 test site in GTT (Torino, Italy) is shown.

The upper level of system hierarchy after the single cell is the cell bundle, which consists of a 24-cell array arranged as 8 cells in electrical series by 3 cells in electrical parallel. Four cell bundles are connected in series to form a bundle row, and 12 bundle rows are aligned side by side, interconnected in serpentine fashion with an in-stack reformer between each bundle row (for a total of 1152 single cells). In the following of the paper we refer to a cell sector, which is defined like the electrical serie of two cell bundles. In the new rebuilt a multi-pedigree cell stack has been assembled; SOFC cells mainly differ for total running hours; one of the interest of the experimentation is to study how cell with different operating history work together in a stack. The rest of the system is composed by the balance of plant (BoP), with five major skids: Generator Module, Electrical Control System, Fuel Supply System (FSS), Thermal Management System (TMS), and Heat Export System (HES) [1–6,9–12,15–17].

From the electrical point of view, the module is made up of four parts: (a) the electrochemical generator; (b) the Power Conditioning System (PCS): an inverter, which operates the dc/ac conversion; (c) the SOFC auxiliaries (blowers); (d) the Fuel Cell Board (QFC), designed by Politecnico of Torino, which allows one the electrical connection of the CHP 100 to the grid. From the thermal point of view, the exhausts from the stack, passing in a cross finned tubes gas-water exchanger, provide, in nominal conditions, approximately 60 kW_t of thermal energy, used for the winter and summer conditioning (through a absorption refrigerator cycle water-lithium bromide fed with hot water) of some offices of the GTT factory.

The schematic of the cell stack arrangement is shown in Fig. 2 [17], outlining the position of the fuel ejectors and the power leads. The simplified flow schematic of the SOFC CHP-100 BoP is shown in Fig. 3, with the schematic of the primary generator structure. In Fig. 2, it is shown the position of the fuel ejectors and power leads. In the paper, the results will be discussed dividing ideally the primary generator in four main zones (North; South; Power Leads side and Ejectors side), and also in the central zone (middle between power leads and ejectors side).

The commissioning date in GTT was June 19, 2005. The operational data at September 2006 report a number of run hours in GTT of around 10,000, with a total run hours of around 30,000 (including run hours in the Netherlands and Germany); a average stack temperature of 954 °C; a dc generated power of 123.6 kW_e, at 246.1 VDC and 502.3 A; a ac generated power of 113 kW_e; a power to GTT workshop grid of 103 kW_e (20% of the workshop

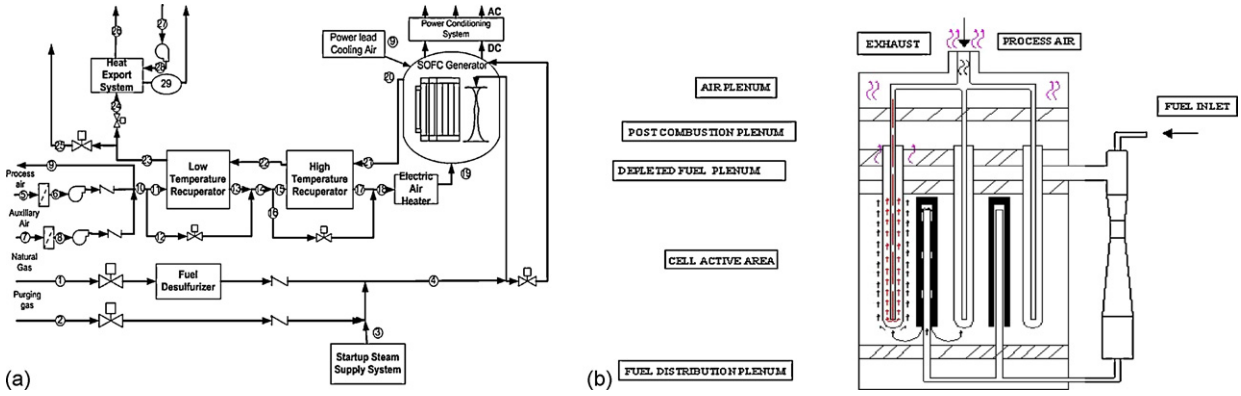

Fig. 3. Simplified flow schematic of the SOFC CHP-100 BoP, and schematic of the primary generator structure.

requirement); a heat generation of 60 kW_t (hot water at 85 °C). Other characteristics are: a reliable operation also with significant LHV changes of the natural gas; no measurable voltage or power degradation; a very high availability of 99.5% (actual, on annual basis); 4 stops (one operation error, three inverter failures); 24 successful operation transition to power dissipator due to utility (AEMD, Azienda Energetica Metropolitana Torino Distribuzione) or GTT grid failures; no thermal cycles; a very dependable automatic operation (no operator in control room); a remote control capability via modem; a easy maintenance (replacement of air filters and of desulphurization reactant). In 1 year of operation the SOFC CHP-100 fuelled by natural gas avoids the production of 272 tonnes of CO_2, the environmental pollution of 1035 kg of NO_x, the import of 121 tonnes of oil equivalent with respect to a gas turbine plant of higher size (in the order of 100 MW_e; therefore, if compared to a similar size gas turbine, the advantage would be even higher). Green Certificates are provided by the Italian Authority (GRTN) for electrical energy produced by a fuel cell generator (also using a fossil fuel): the energy production estimate in 2006 is 900 MWh (18 certificates).

2.2. Description of the experimental sessions

The scheduled tests have been carried out in the November 2005 and March 2006, following the methodology of the Design of Experiments. The main aim has been the characterization of the operation of the single sectors of the system, pointing out the analysis on the behavior of the local temperatures and voltages.

Four factors were investigated at the nominal load operation: the fuel consumption FC, the air stoichs λ_{air}, the setpoint temperature T_{GEN}, and the air pre-heating temperature T_{air}. The most significant factors affecting the generator behavior are the fuel consumption FC, the air stoichs λ_{air}.

The fuel utilization (FU) factor is defined as the ratio of the fuel mass flow that operates the electrochemical oxidation on the anode surface, to the total fuel mass flow that enters the generator. The control variable fuel consumption (FC) factor is defined in the same way, but, at the numerator it also takes into account the fuel mass flow that is chemically oxidized on the anode side due to the air leakage from the cathode to the anode through the electrolyte layer or other sources (of the order of 20–30 $cm^3\ min^{-1}$ at 300 mA cm^{-2} according to [13]), plus the fuel by-pass through the insulation package.

The air stoichs factor (λ_{air}) is defined as the ratio of the total air mass flow which enters in the generator and the air mass flow operating in the electrochemical reaction on the cathode surface.

The generator setpoint temperature (T_{GEN}) is the higher measured temperature by the five thermocouples placed in the central zone of the generator.

The air pre-heating temperature (T_{air}) is the temperature of the process air after its heating in the thermal management system of the balance of plant and before entering the generator canister.

In order to ensure a safe operation of the generator, the investigated experimental domain has been in the range of: $81.75\% < FC < 84.25\%$ and $4.6 < \lambda_{air} < 4.8$, moreover, the average current density has been kept constant at the nominal value of 0.2 A cm^{-2} (500 A generator current).

The investigated dependent variables focused on the distribution in the generator of voltages and temperatures (average temperatures of the generator in different planes: total stack thermocouples, top plane thermocouples, middle plane thermocouples and bottom plane thermocouples). From an electrical point of view it is possible to acquire the generator terminal voltage and the voltage of two bundles in series (sector).

Once the setpoint was established, the data collection started after 60 min (to stabilize the signal data) for a period of 30 min, with a rate of 1 min. The single value of a variable is the mean value of the 30 values collected in every test length. To develop the study, the factorial analysis and the response surface method (RSM) have been applied, and first and second-order regression models linking the dependent variable to the control factors have been found and analyzed with an ANOVA. In many physical or engineering problems two or more variables are related and it is of interest to model and explore this relationship. Suppose that there is a single dependent variable or response Y that depends on k independent or regressor variables, for example $x_1, x_2, \ldots, x_3$. The relationship between these variables is characterized by a mathematical model, called a regression model, that is fit to a set of sample data. In some instances, the experimenter knows the exact form of the true functional relationship between Y and $x_1, x_2, \ldots, x_k$.

However, in most cases, the true functional relationship is unknown and the experimenter can choose an appropriate function in order to approximate it. Low-order polynomial models are widely used as approximating functions. Thus, a regression model can be written in the following form:

$$Y = \beta_0 + \beta_1 x_1 + \beta_2 x_2 + \ldots + \beta_k x_k + \varepsilon \quad (1)$$

is called a multiple linear regression model with k regressor variables. The parameters β_j ($j = 0, 1, \ldots, k$) are called the regression coefficients. The parameter β_j represents the expected change in response Y per unit change in x_j when all the remaining independent variables x_i ($i \neq j$) are held constant. Thus, the regression coefficient of a regressor variable is the sensitivity parameter of the dependent variable to changes in the regressor variable (independent variable).

The method of least squares is typically used to estimate the regression coefficients in a multiple linear regression model. If an experimental session is designed by applying the methodology of the Design of Experiments then the investigated dependent variables can be described by regression models. Different forms of regression models can be obtained from an experimental session according to the chosen design of experiments, for example first (Eq. (1)) or second-order regression models:

$$Y = \beta_0 + \sum_{j=1}^{k} \beta_j x_j + \sum \sum_{i<j} \beta_{ij} x_i x_j + \sum_{j=1}^{k} \beta_{jj} x_j^2 + \varepsilon \quad (2)$$

Because of the reduced experimental domain of this analysis we will deal with results obtained by a first-order design.

The data have been first analyzed through the Yate's method (analysis of the factor significance on the dependent variable); after, first and second-order regression models have been obtained. Particular attention has been addressed in the description of the operation in terms of sensitivity maps. The analysis is described in the following paragraphs.

3. Results

3.1. Sensitivity of the voltage distribution to fuel consumption and air stoichs

In this paragraph the results of the sensitivity analysis of local voltages to fuel consumption and air stoichs are shown. As said in the last paragraph, the coefficients of the regression models represent the sensitivity coefficients of the analyzed dependent variable to the factor. In this case the coefficients are expressed in V/%FC and V/%stoichs, being the FC and λ_{air} factors the global values (inputs of the operator).

In order to better understand the discussion about sensitivity to fuel utilization tests some results are presented about the voltage distribution in the stack and the polarization behavior [18]. In Fig. 4 (non-disclosure agreement with Siemens) the voltage distribution in the stack sectors is shown for the following operating condition ($I = 435$ A, setpoint temperature $T_{GEN} = 967\,^{\circ}C$, FC = 84.25%). In Fig. 5 a short polarization (from $I = 435$ to 475 A) is shown.

The average cell voltage is around 666 ± 14 mV, and the estimated average area specific resistance is around $1.04 \pm 0.08\ \Omega\,cm^2$, comparable with other works [16,19]. The performance homogeneity (obtained by the estimated standard deviation) of the single cell voltage is then 2%, which is a very good index of the operation; during different experimental sessions, values of performance homogeneity of the single cell voltage have been found up to 5%. It is also evident that the edges' sectors show a lower terminal voltage.

In Fig. 6 the sensitivity of the voltage of a sector (group of 16 cells in electrical series) to fuel consumption is shown. The average sector sensitivity is -44 mVsector/%FC. The increase of the fuel consumption leads to a significant decrease of voltage in all the stack's sectors, mainly because of the reduction of the average Nernst potential and the increase of diffusion overvoltages. The shape of the sensitivity voltage distribution in the bundle rows is parabolic, with a minimum in the central zone of the generator: the sectors placed at the edges have very high sensitivity to FC, in particular the sectors placed at the generator' corners of the ejectors' side.

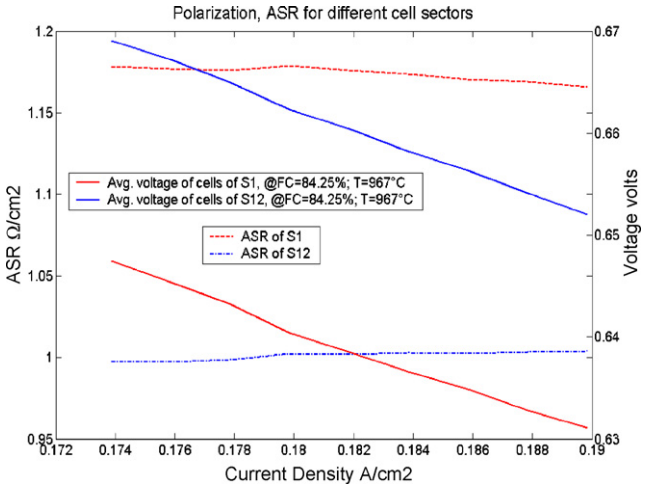

Fig. 5. Polarization behavior of two stack's sectors.

In Fig. 7 the sensitivity of the sector voltage to the air stoichs is shown. The average sector sensitivity is around -20 mVsector/0.1 stoichs. The increase of the air stoichiometry, λ_{air} leads to a significant decrease of voltage in all the sectors (except for the ones placed at the generator's edges: but we have evaluated that the effect is statistically not significant). Note that the central zone of the generator shows a maximum of sensitivity of voltage to air stoichiometry: it is interesting to notice the parabolic shape of the sensitivity distribution along

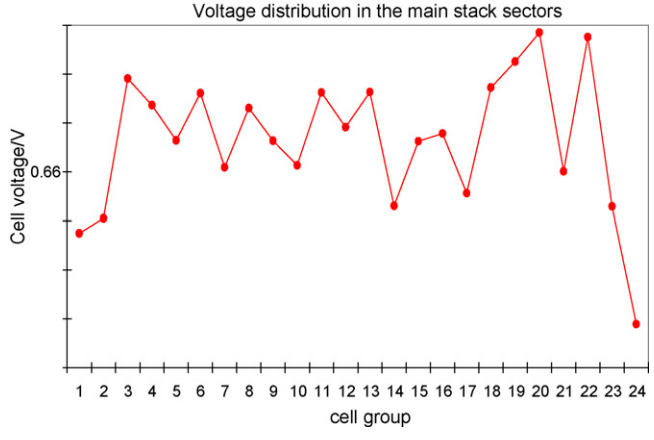

Fig. 4. Voltage distribution in the main stack's sectors.

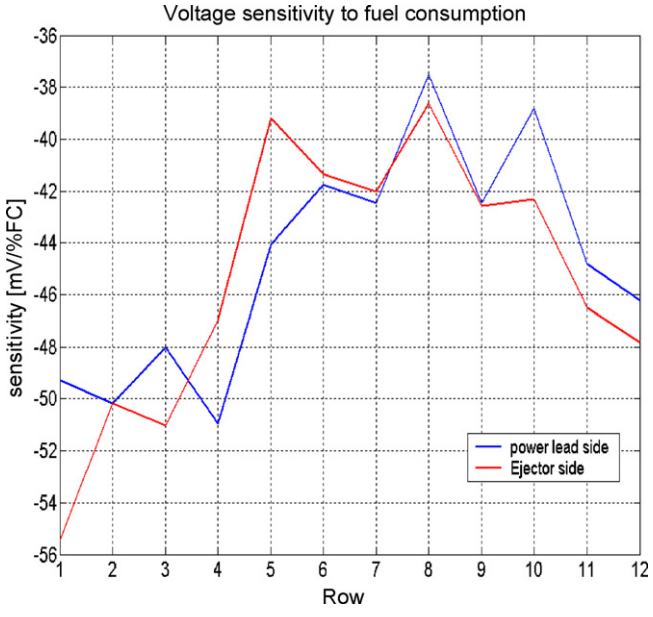

Fig. 6. Sensitivity of the sectors' voltage to fuel consumption.

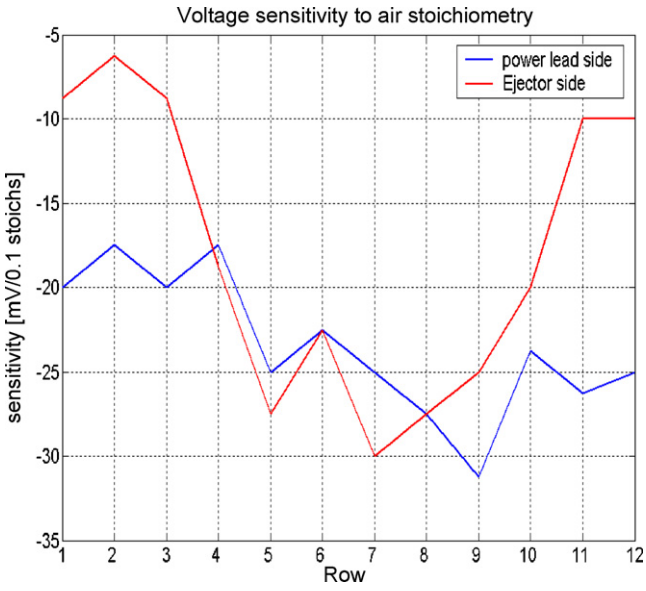

Fig. 7. Sensitivity of the sectors' voltage to air stoichs.

the bundle rows and the complementary behavior between the air stoichs and the FC sensitivity.

As the SOFC CHP-100 is an air-cooled system, the decrease of voltage, due to an increase of air stoichiometry, is mainly due to the variation of the equilibrium temperature: an increase of λ_{air} causes a reduction of the equilibrium temperature with consequent increase of overvoltages (mainly ohmic contribution). This decrease of the temperature is almost uniform in all the bundle rows of the generator (the discussion is addressed in the next paragraph), then also at the edges. Thus, it would be expected that also the edge sectors will present the same behavior, that is a reduction of voltage with increasing of λ_{air}. The negligible effect of this operation on these sectors is explained with the hypothesis that it is the local fuel consumption the dominant factor of the operation in the edge sectors.

The last consideration concerns the linear dependence between voltage and temperature expressed by the obtained regression models. Through the statistical analysis it was evaluated that the first-order regression had a good fit (reduce lack of fit value). But from a physical point of view, the linear behavior is not expected and the performance is expected to be an exponential dependence of operating temperature. In fact, the solid oxide fuel cell behavior can be estimated by the Arrhenius expression as this is the behavior of ionic and electronic conductivities of the cell layers [20]. Therefore, the linear dependence is explained with the small variation of the experimental domain for temperature (953 °C at $\lambda_{air} = 4.6$ and 944 °C at $\lambda_{air} = 4.8$).

Looking at Fig. 8, it is interesting to notice the distribution along the bundle rows of the voltage sensitivity of the single cell to both fuel consumption and air stoichiometry, outlined for cells placed at the ejectors and power leads' sides.

The estimation of the single cell sensitivity to fuel consumption is around −2.8 mVcell/%FC, comparable with other works

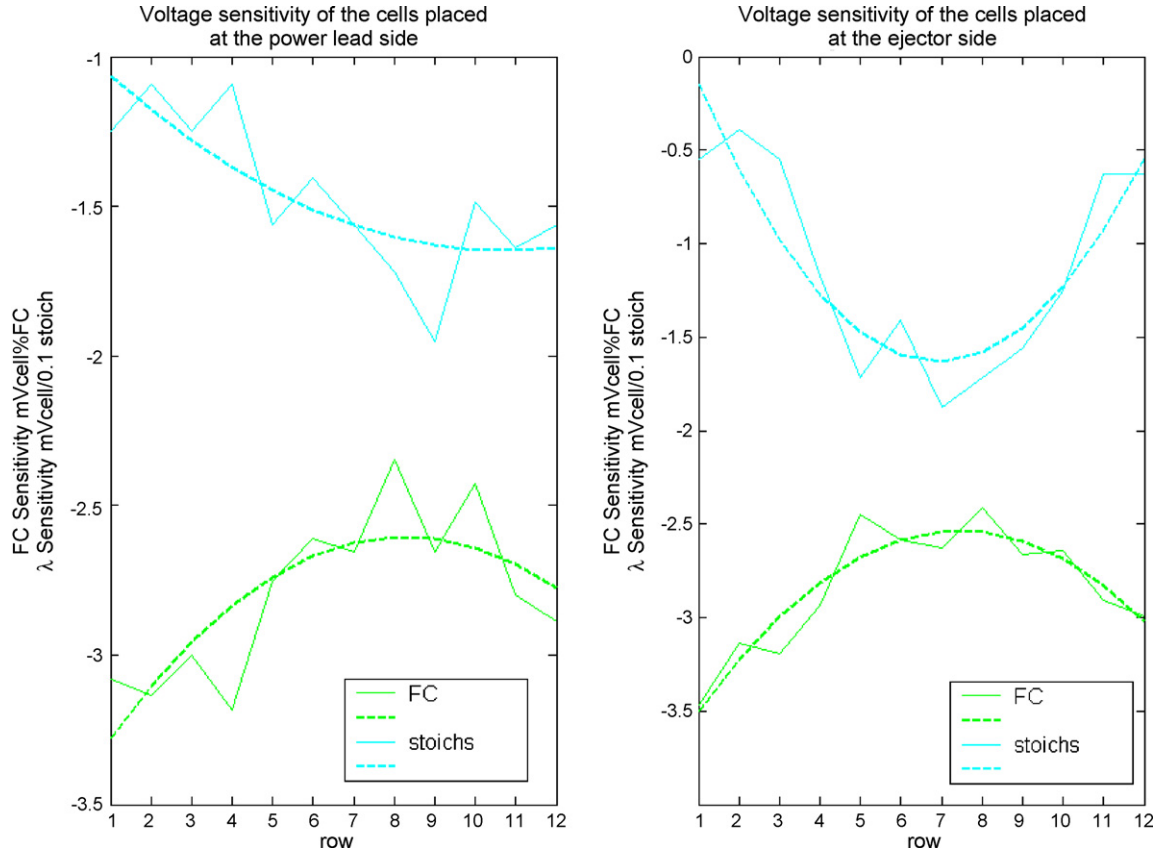

Fig. 8. Voltage sensitivity to the factors of the single cells along the bundle rows.

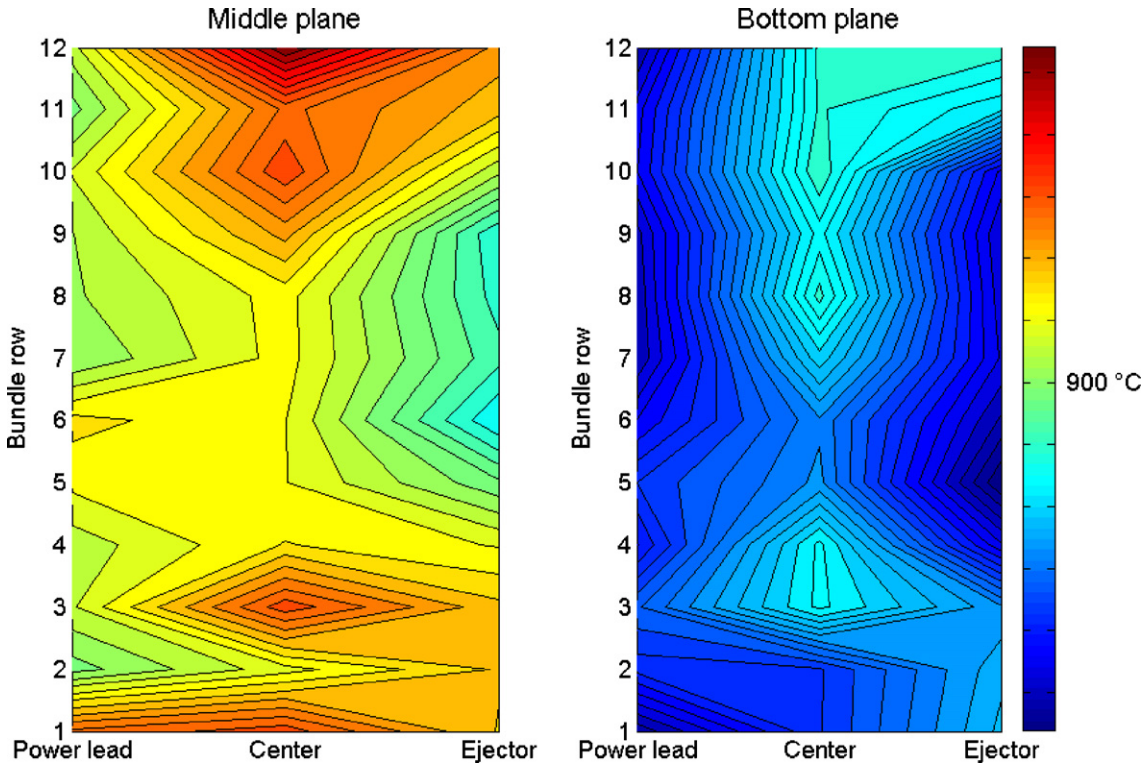

Fig. 9. Temperature distribution along the bundle rows.

[13]; the homogeneity of the FC sensitivity among the various cells is around 10%. The single cell sensitivity to air stoichiometry has been estimated in around −1.3 mVcell/%0.1 stoichs. Also from this figure it is clear that the higher is the FC sensitivity the lower is the sensitivity to the air stoichiometry. Moreover, the distribution of FC sensitivities is used in the following of the paper in order to estimate the local fuel utilization of the cell sectors.

3.2. Sensitivity of the temperature distribution and profiles to fuel consumption and air stoichs

In this paragraph the results of the sensitivity analysis of temperature distribution to fuel consumption and air stoichs are shown. The coefficients of the regression models, that represent the sensitivity coefficients of the analyzed dependent variable to the factor, are expressed in °C/%FC and °C/%stoichs.

In Fig. 9 (non-disclosure agreement) the distribution of temperatures in the stack is shown, taking into account two measurement planes: the bottom plane (corresponding to the closed end of tubular cell and to the fuel inlet) and the middle plane. With respect to the middle plane temperature, the highest temperatures are measured in the central zone and at the border of the stack with a cooling effect at the fuel ejectors' side; the temperature gradient is more than 100 °C [21].

In order to better understand the discussion about the sensitivity analysis, some results about the axial shape of temperature along the tubular cell are also presented. In Fig. 10 (non-disclosure agreement), the typical axial temperature profile is shown (at $T_{air} = 612\,^{\circ}C$ and $\lambda_{air} = 4.6$, $i_c = 200\,mA\,cm^{-2}$, FC = 84.25%). The average top plane temperature is around 860 °C, the average middle plane temperature is around 930 °C and the bottom plane temperature is around 840 °C. The low temperature at the closed end of the cell (corresponding of the fuel inlet condition) is explained by the residual reforming endothermic reaction which takes place at the cell anode surface [22].

In Fig. 11 the sensitivity of the local temperature to air stoichiometry is shown for the two investigated measurements planes (bottom and middle plane). The regulation of the air stoichiometry affects the thermal equilibrium of cells; an increase of λ_{air} leads to a reduction of temperature and the effect is stronger at the middle plane (in the figure the results are presented in absolute value). Moreover, the central zone of the stack is greatly affected by this regulation, due to the design of the air distribution plenum. Nevertheless, we observe that the sensitivity of the

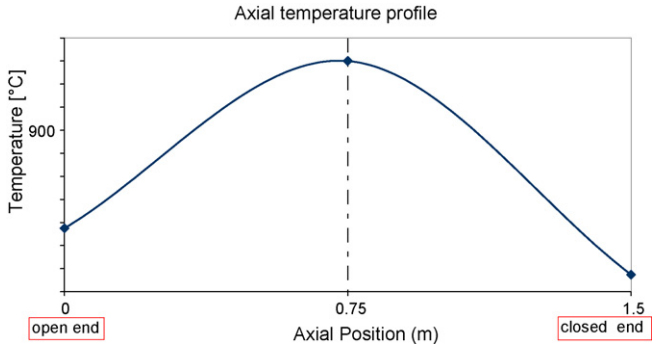

Fig. 10. Axial temperature profile of a tubular SOFC.

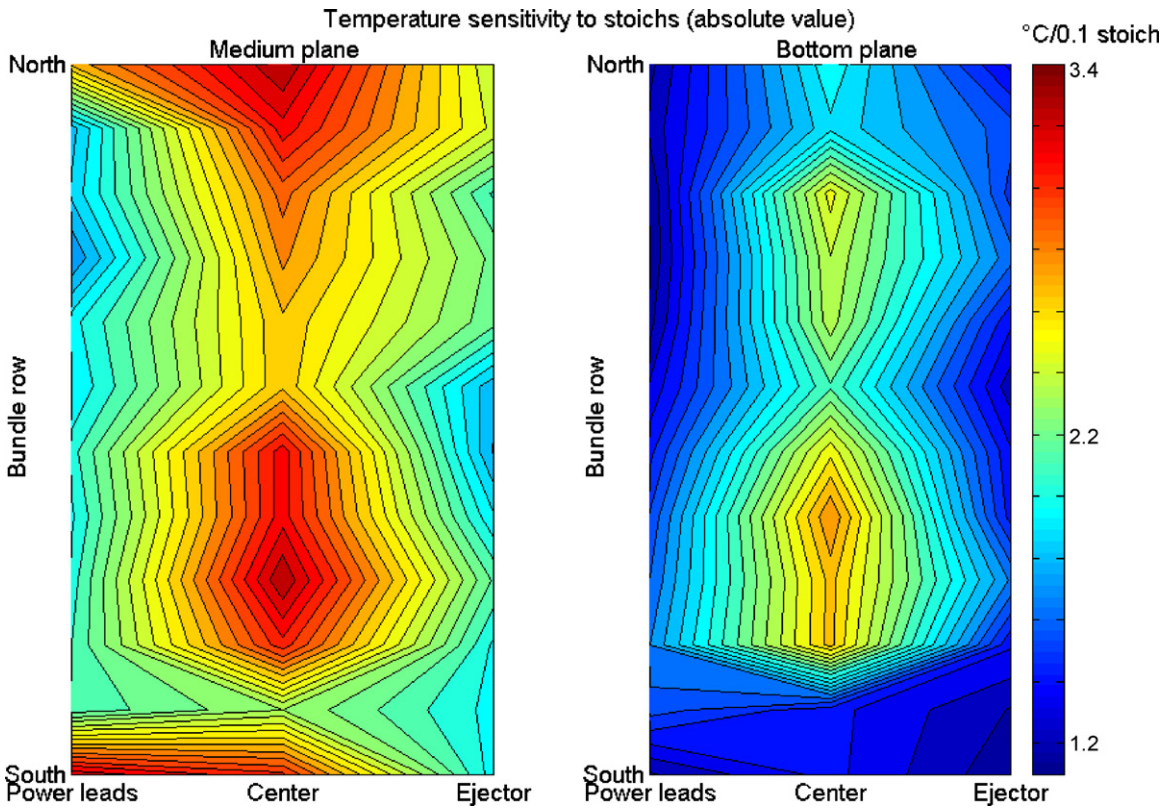

Fig. 11. Sensitivity of local temperature to air stoichiometry.

local temperature is almost uniform along the bundle rows: this point will be discussed later on.

In Fig. 12 the sensitivity of the local temperature to fuel consumption is shown. The effect is negative (in figure the absolute values are reported): it is interesting to notice how the middle plane temperature is slightly affected by the operation, while the bottom plane temperatures seem to be affected by variations on FC values. The test has been performed at fixed setpoint temperature. This means that the increase of FC would lead to a stack heating (due to irreversibility), but due to the imposed setpoint temperature, an higher air mass flow is sent to the stack with the final effect that middle plane temperatures do not change (in the middle plane is located the thermocouple which measures the setpoint temperature) while a decrease of temperature is measured in the bottom zone of cells.

4. Deduction of the local fuel utilization distribution

Experiments about sensitivity to fuel utilization form an important feature of testing solid oxide fuel cell systems. In this paragraph we describe the sensitivity to fuel utilization tests performed on the SOFC CHP-100 stack and its relation to the local fuel utilization of the cell sectors. In fact, the local fuel utilization of cell sectors can be estimated coupling experimentally performed sensitivity to fuel utilization tests with a proposed model of cell voltage sensitivity to fuel utilization.

The following results were obtained from the experimental analysis: stack terminal voltage sensitivity −1.06 V/%FC; cell sectors sensitivity −44 mVsector/%FC; single cell sensitivity −2.8 mVcell/%FC. It has been shown in Fig. 8 that the homogeneity of the FC sensitivity among the various cells is around 10%. The different behavior of the sensitivity is mainly addressed to the local fuel utilization operation, so to the design of the fuel distribution system. In order to deduce the local fuel utilization a model of cell voltage sensitivity to FU has been developed.

The sensitivity of cell voltage to fuel utilization depends on several contributions which concern the Nernstian term, the contribution of diffusion term and eventually the effect of leakages of air at the anode side. It is neglected the ohmic contribution, the activation contribution is also neglected because of its small effect of the voltage drop. If the performance of a cell is limited by the ohmic contribution and leakages can be neglected then the sensitivity of cell terminal voltage to FU is well described by the variation of Nernstian term with fuel utilization. In the case of a tubular cathode supported cell the performance is also limited by cathodic diffusion and leakages play an important rule [13]. In the following some considerations are made about all these terms.

The terminal voltage of a tubular SOFC is expressed by the equation:

$$V_c = V_{Nernst} - \eta_{act,a/c} - \eta_{ohm} - \eta_{conc,a/c} \quad (3)$$

where V_c is the terminal voltage, V_{Nernst} the Nernst voltage, $\eta_{act,a/c}$ the activation overpotential, η_{ohm} the ohmic overpotential, $\eta_{conc,a/c}$ is the concentration overpotential.

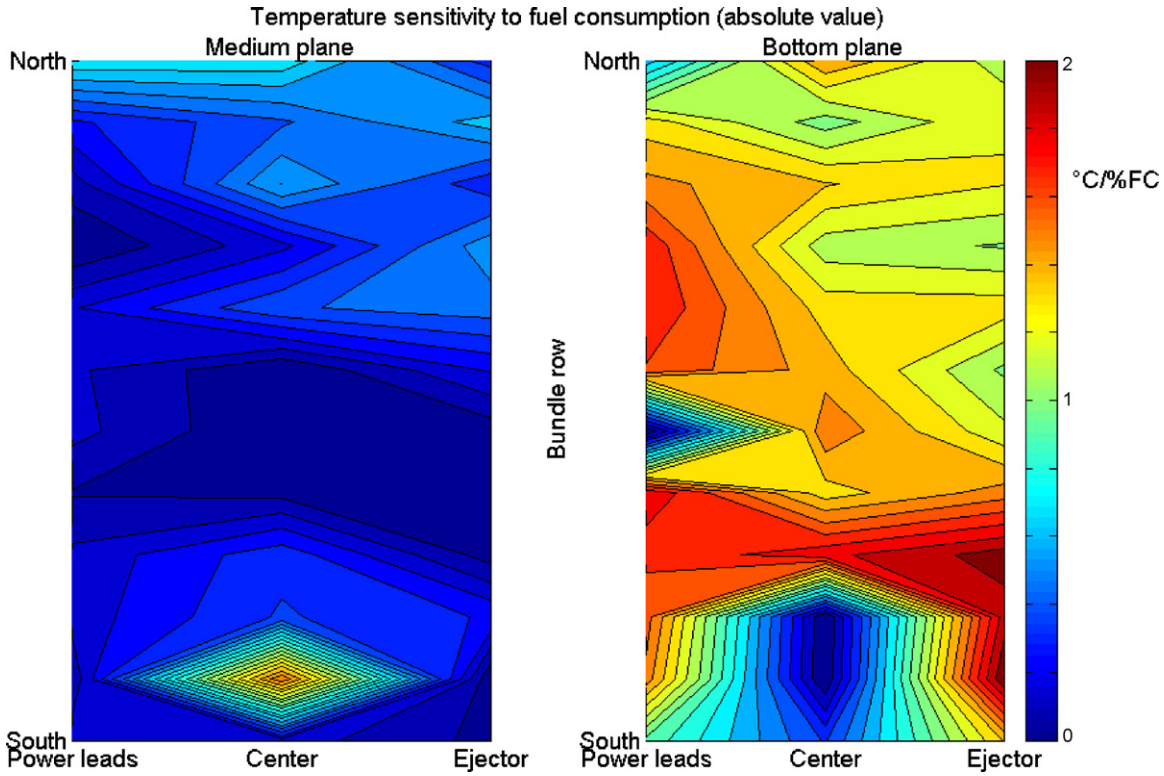

Fig. 12. Sensitivity of local temperature to fuel consumption.

The Nernst voltage is expressed, with the hypothesis of ideal gas, by the following equation:

$$V_{\text{Nernst}} = E_0 + \frac{RT}{2F}\ln\left(\frac{(y_{\text{H}_2})(y_{\text{O}_2})^{1/2}}{(y_{\text{H}_2\text{O}})}\right) \tag{4}$$

Under the assumption that the oxygen utilization is negligible, that is the oxidant is fed to the cell far in excess of the stoichiometrically required amount, the Nernst voltage is a function of the operating temperature and of the axial location along the cell length, at fixed pressure:

$$V_{\text{Nernst}}(x, T) = E_0(T) + \frac{RT}{2F}\ln\left(\frac{(y_{\text{H}_2}(x))(y_{\text{O}_2})^{1/2}}{(y_{\text{H}_2\text{O}}(x))}\right) \tag{5}$$

The average Nernst potential is the position averaged Nernst potential, that is:

$$\bar{V}_{\text{Nernst}} = \frac{1}{L}\int_0^L V_{\text{Nernst}}(x)\,\text{d}x \tag{6}$$

Basing on the papers [13,22], it is shown that the sensitivity of voltage to FU is depending on the average current density due to the variation of the consumption of reactants along the cell axis with current: the sensitivity decreases with the increase of current. In order to model this behavior some assumptions are now made. At high current densities it can be assumed that the Nernst voltage is linear with the cell axial position:

$$V_{\text{Nernst}}(x, T) = E_0(T) + \frac{RT}{2F}\ln\left(\frac{(y_{\text{H}_2}(x))(y_{\text{O}_2})^{1/2}}{(y_{\text{H}_2\text{O}}(x))}\right) = \text{A}x + \text{B} \tag{7}$$

This refers to an operation with exponential variation of the reactants' partial pressure along the cell length according to the equation:

$$y_i(x) = y_i(0)\,\text{e}^{((1/L)\log(y_i(L)/y_i(0)))x} \tag{8}$$

The boundary conditions are assumed by knowing the fuel composition at the cell inlet, in terms of hydrogen and water vapour molar fractions, and the fuel utilization, this allows one to find the A and B coefficients.

At $x = 0$ (closed end), that is at the cell inlet, it can be written:

$$\begin{aligned} y_{\text{H}_2}(0) &= y^0_{\text{H}_2} \\ y_{\text{H}_2\text{O}}(0) &= y^0_{\text{H}_2\text{O}} \end{aligned} \tag{9}$$

in the fuel mixture (anode inlet composition).

At $x = L$ (open end), that is at the cell outlet it can be written:

$$\begin{aligned} y_{\text{H}_2}(L) &= y^0_{\text{H}_2}(1 - \text{FU}) \\ y_{\text{H}_2\text{O}}(L) &= y^0_{\text{H}_2\text{O}} + y^0_{\text{H}_2}\text{FU} \end{aligned} \tag{10}$$

The position averaged Nernst voltage at high current densities is written in the form:

$$\bar{V}_{\text{Nernst,HC}}(T) = E_0(T) + \frac{RT}{4F}\ln\left(\frac{\left(y_{\text{H}_2}(1 - \text{FU})\right)\left(y_{\text{O}_2}\right)^{1/2}}{\left(y_{\text{H}_2\text{O}} + y_{\text{H}_2}\text{FU}\right)}\right) \tag{11}$$

At low current densities, a significant length of the cell would be operating close to the exit Nernst potential, that is most of the fuel will be consumed very close to the fuel inlet, which is the closed end of the cell. The Nernst voltage would decrease

sharply from the inlet value to the exit value to the exit value within a short length from the inlet. At low current densities, the average Nernst potential can be approximated to that of the exit Nernst potential, then constant along the cell tube:

$$\bar{V}_{\mathrm{Nernst,LC}}(T) = E_0(T) + \frac{RT}{2F}\ln\left(\frac{(y_{\mathrm{H_2}}(1-\mathrm{FU}))(y_{\mathrm{O_2}})^{1/2}}{(y_{\mathrm{H_2O}} + y_{\mathrm{H_2}}\mathrm{FU})}\right) \tag{12}$$

Neglecting the diffusion term and the leakages the sensitivity of the cell voltage to the fuel utilization can be assumed to be equal to the sensitivity of the Nernst voltage to the same parameter. With this assumption it is possible to write:

$$\frac{\mathrm{d}V_{\mathrm{c}}}{\mathrm{dFU}} = \frac{\mathrm{d}V_{\mathrm{Nernst}}}{\mathrm{dFU}} \tag{13}$$

With this assumption the derivative of the terminal voltage with respect to the fuel utilization, equal to the sensitivity to the fuel utilization, at low current densities is twice the one at high current densities, in fact at high current density the sensitivity is given by the Eq. (14), while at low current density it is given by the Eq. (15).

$$\left.\frac{\partial \bar{V}_{\mathrm{Nernst}}}{\partial \mathrm{FU}}\right|_{\mathrm{HC}} = -\frac{RT}{4F}\left[\frac{1}{(1-\mathrm{FU})(y^0_{\mathrm{H_2O}} + y^0_{\mathrm{H_2}}\mathrm{FU})}\right] \tag{14}$$

$$\left.\frac{\partial \bar{V}_{\mathrm{Nernst}}}{\partial \mathrm{FU}}\right|_{\mathrm{LC}} = -\frac{RT}{2F}\left[\frac{1}{(1-\mathrm{FU})(y^0_{\mathrm{H_2O}} + y^0_{\mathrm{H_2}}\mathrm{FU})}\right] \tag{15}$$

If the oxygen utilization would be taken into account then the Eqs. (14) and (15) will be modified according to (i.e. on Eq. (15)):

$$\frac{\partial \bar{V}_{\mathrm{N}}}{\partial \mathrm{FU}} = -\frac{RT}{2F}\left[\frac{1}{(1-\mathrm{FU})(y^0_{\mathrm{H_2O}} + y^0_{\mathrm{H_2}}\mathrm{FU})} + \frac{1}{2}\frac{(\lambda/y^0_{\mathrm{O_2}}) - \lambda}{(\lambda - y^0_{\mathrm{H_2}}\mathrm{FU})((\lambda/y^0_{\mathrm{O_2}}) - y^0_{\mathrm{H_2}}\mathrm{FU})}\right] \tag{16}$$

Because of the partial pressure of the oxygen at the cathode exit can be written as [16]:

$$y_{\mathrm{O_2}} = \frac{\lambda - \mathrm{FU}y^0_{\mathrm{H_2}}}{(\lambda/y^0_{\mathrm{O_2}}) - \mathrm{FU}y^0_{\mathrm{H_2}}} \tag{17}$$

In the case of the tested air stoichiometry values, λ 4.6/4.8, this effect can be neglected on the sensitivity curve. This relation involves a definition of air excess different than the one used in the paper (such values are higher than ones tested experimentally, see ref. [16]), thus all considerations discussed in the paper represent a conservative situation and the discussion is only deepen for a comprehensive analysis of all polarization terms.

To refine the model some considerations about the effect of fuel utilization on the diffusion losses are now discussed. The analyzed cell is a cathode-supported cell then the main effect of diffusion is mainly addressed to the cathodic layer. The model equations and hypothesis are assumed by literature [22,23]. Transport of gaseous species usually occurs by binary diffusion, where the effective binary diffusivity is a function of the fundamental binary diffusivity $D_{\mathrm{H_2}}$–$D_{\mathrm{H_2O}}$ and microstructural parameters of the anode. In electrode microstructures with very small pore size, the possible effects of Knudsen diffusion, adsorption/desorption and surface diffusion may also be present. In terms of physical measurable parameters, an analytical expression for anodic concentration polarization is proposed. This equation is:

$$i_{\mathrm{as}} = \frac{2Fp^{\mathrm{b}}_{\mathrm{H_2}}(\mathrm{FU})D_{\mathrm{a(eff)}}}{RTt_{\mathrm{a}}} \tag{18}$$

It is obtained by posing to zero the following equation:

$$p^{\mathrm{a}}_{\mathrm{H_2}} = p^{\mathrm{b}}_{\mathrm{H_2}}(\mathrm{FU}) - \frac{RTt_{\mathrm{a}}}{2FD_{\mathrm{a(eff)}}}i_{\mathrm{c}} \tag{19}$$

Where the pressure of fuel at the bulk depends on fuel utilization operation.

The voltage drop due to the anodic diffusion is given by:

$$V^{\mathrm{a}}_{\mathrm{diff}} = \frac{RT}{2F}\log\left(1 - \frac{i}{i_{\mathrm{as}}}\right) \tag{20}$$

In terms of physical measurable parameters, the cathode-limiting current density can be evaluated in the form:

$$i_{\mathrm{cs}} = \frac{4Fp^{\mathrm{b}}_{\mathrm{O_2}}D_{\mathrm{c(eff)}}}{((p - p^{\mathrm{b}}_{\mathrm{O_2}})/p)RTt_{\mathrm{c}}} \tag{21}$$

This equation is an approximation for anode supported cells with very small cathode thickness. In general the limiting current at the cathode is given by posing to zero the equation:

$$p^{\mathrm{c}}_{\mathrm{O_2}} = p - (p - p^{\mathrm{b}}_{\mathrm{O_2}}(\lambda, \mathrm{FU}))\,\mathrm{e}^{(RTt_{\mathrm{c}}/4FpD_{\mathrm{c(eff)}})i_{\mathrm{c}}} \tag{22}$$

Where the partial pressure of the oxidant at the bulk depends on fuel utilization and air stoichiometry (Eq. (17)).

The voltage drop due to the cathodic diffusion is given by:

$$V^{\mathrm{c}}_{\mathrm{diff}} = \frac{RT}{4F}\log\left(1 - \frac{i}{i_{\mathrm{cs}}}\right) \tag{23}$$

In this way the drop of voltage due to a variation of fuel utilization is modeled also considering the effect on the cathodic diffusion. The effect of diffusion on the terminal voltage sensitivity of fuel utilization has significant effect when the limiting current density is approached or for low value of the air stoichiometry.

It is possible to write with respect to Eqs. (20) and (23):

$$\frac{\partial \bar{V}^{\mathrm{a}}_{\mathrm{diff}}}{\partial \mathrm{FU}} = \frac{RT}{2F}\frac{1}{1-(\bar{i}_{\mathrm{c}}/\bar{i}_{\mathrm{as}})}\left(\frac{\bar{i}_{\mathrm{c}}(\partial \bar{i}_{\mathrm{as}}/\partial \mathrm{FU})}{\bar{i}^2_{\mathrm{as}}}\right) = \frac{RT}{2F}\frac{\bar{i}_{\mathrm{c}}}{(\bar{i}_{\mathrm{as}} - \bar{i}_{\mathrm{c}})\bar{i}_{\mathrm{as}}}\frac{\partial \bar{i}_{\mathrm{as}}}{\partial \mathrm{FU}} \tag{24}$$

$$\frac{\partial \bar{V}^{\mathrm{c}}_{\mathrm{diff}}}{\partial \mathrm{FU}} = \frac{RT}{4F}\frac{1}{1-(\bar{i}_{\mathrm{c}}/\bar{i}_{\mathrm{cs}})}\left(\frac{\bar{i}_{\mathrm{c}}(\partial \bar{i}_{\mathrm{cs}}/\partial \mathrm{FU})}{\bar{i}^2_{\mathrm{cs}}}\right) = \frac{RT}{4F}\frac{\bar{i}_{\mathrm{c}}}{(\bar{i}_{\mathrm{cs}} - \bar{i}_{\mathrm{c}})\bar{i}_{\mathrm{cs}}}\frac{\partial \bar{i}_{\mathrm{cs}}}{\partial \mathrm{FU}} \tag{25}$$

Table 1
Parameters used in the modeling of the diffusion overvoltages

Parameter	Anode	Cathode
$D_{a/c(eff)}$, effective binary diffusivity	$D_{a(eff)} = (\varepsilon/\tau)D^{293\,K}_{H_2-H_2O}(T/293)^{1.5}$	$(\varepsilon/\tau)D^{293\,K}_{O_2-N_2}(T/293)^{1.5}$
$D_i - D_j$, fundamental binary diffusivity ($cm^2\ s^{-1}$)	$D^{293\,K}_{H_2-H_2O} = 0.91$	$D^{293\,K}_{O_2-N_2} = 0.22$
ε	0.3	0.335
τ	3	5

It should be noted that:

$$\frac{\partial \bar{V}^{a/c}_{diff}}{\partial FU} \propto \frac{1}{D_{a/c(eff)}} \quad (26)$$

$$\frac{\partial \bar{V}^{a/c}_{diff}}{\partial FU} \propto t_{a/c} \quad (27)$$

The effect of the diffusion on the sensitivity of voltage to the fuel utilization is inversely proportional to the effective binary diffusivity on the electrodes' layers and directly proportional to the electrodes' thickness.

The parameters used for solving the equations have been listed in Table 1.

An important role is played by eventual leakages of air at the anode side; in fact some fuel can burn with the oxidant with the consequence that it does not react at the anode surface to generate current. If it would occur then the effective operational fuel utilization will be higher than the expected and sensitivity to change in FU will be very high approaching high values of fuel utilization.

The results of modeling are shown in Fig. 13. The simplified model refers to the sensitivity model of Nernst voltage to fuel utilization whereas the complete model accounts also for the effect of diffusion and leakages (3% of leakages).

The effect of the operating current on the fuel utilization sensitivity is more effective when working at low fuel utilization. At low current the fuel utilization sensitivity is governed essentially by the variation of the average Nernst voltage with FU whereas at high current the effect of diffusion and leakages becomes more effective. The curves are drawn for an operating condition of 1000 °C and for a fuel with 89% H_2 and 11% H_2O of composition. In Fig. 14 some experimental results of single cell sensitivity are reported according to [13].

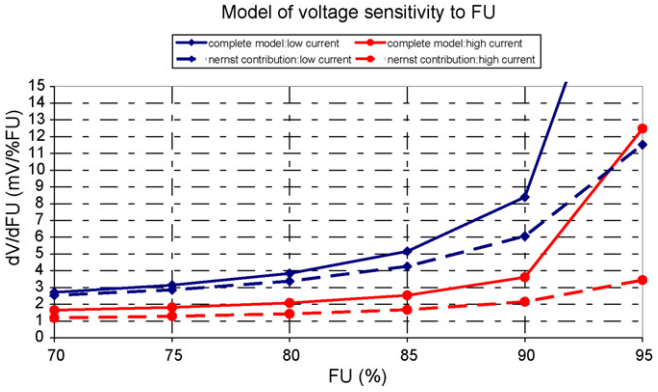

Fig. 13. Model of fuel utilization sensitivity for a tubular SOFC.

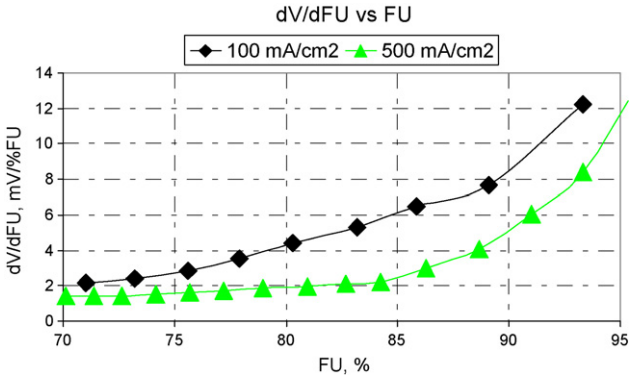

Fig. 14. Experimental data of single cell sensitivity.

Once the model is developed, it can be used in order to explain the different values of local sensitivity to fuel utilization and to analyse the shape of its distribution along the stack sectors (estimated experimentally through the statistical analysis). The distribution of fuel utilization sensitivity (according to the proposed model) depends on the local temperature in the bundle rows, on the fuel inlet condition at the anode in terms of hydrogen and water vapour partial pressures, and on the local fuel utilization. The effect of the local temperature is taken into account in the analysis, the effect of the fuel inlet conditions is taken into account but the strong hypothesis is that the fuel composition is the same for all the bundle rows, that is there is the same reformation degree in all the in-stack standard reformation boards. Once the temperature and the fuel inlet condition are fixed for all the cell sectors, then the local fuel utilization can be estimated by solving the voltage sensitivity model in terms of fuel utilization. The condition of the inlet fuel has been posed to $y_{H_2} = 0.4$ and $y_{H_2O} = 0.2$. The results of the estimation procedure are shown in Fig. 15; the higher is the local FU sensitivity the higher is

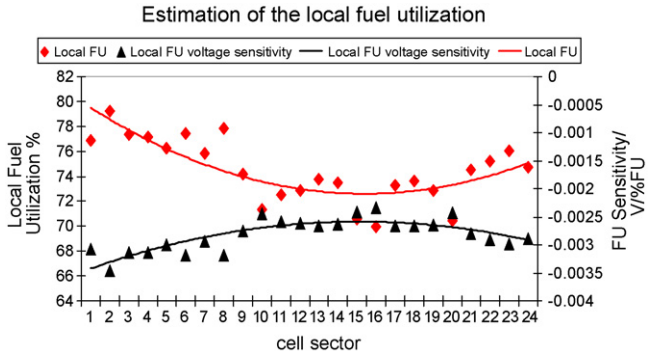

Fig. 15. Estimation of local fuel utilization.

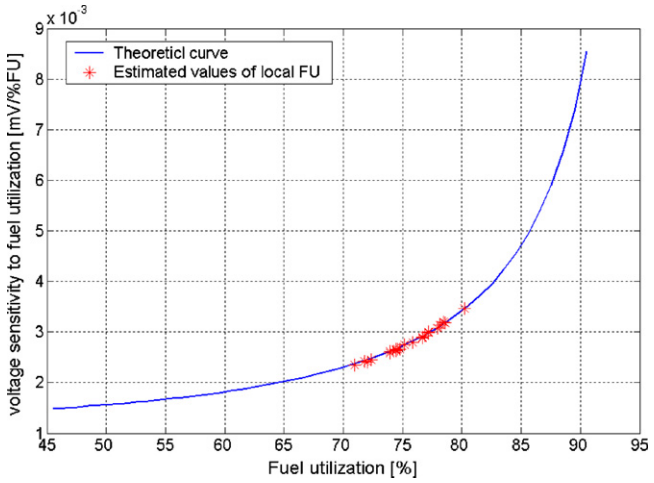

Fig. 16. Model of FU voltage sensitivity vs. estimated local fuel utilization.

the local fuel utilization, the boundaries of the generator work at high fuel utilization, and this can also explain the lower voltages observed at the edge's sectors.

In Fig. 16 the deduced local fuel utilization with the FU sensitivity model used for the estimation are compared.

The model expresses the FU voltage sensitivity at the nominal current of $i_c = 200\,\text{mA cm}^{-2}$. It is shown that the difference of local fuel utilization of cell sectors can differ also for 10% of values.

5. Air stoichs regulation to avoid local overheating: some problems

The model discussed in Section 4 has been used to understand why there is a distribution of voltage sensitivities to FC in the stack as shown in Fig. 6, and to deduce the local FU distribution in the various sectors of the stack: the higher is the sensitivity to fuel utilization the higher is the estimated local fuel utilization. The distribution of the local FU value in the 12 rows of the generator is therefore shown in Fig. 17 (non-disclosure agreement).

The distribution shows higher values of local FU in the boundary rows of the generator, and lowest (better) values in the center rows. This is probably due to the fuel gas distribution in the generator rows and to the operation of the boundary reformation boards: it seems that in the boundary rows a lower amount of fuel gas arrives and the operation is characterized by a local FU factor higher than the overall one. For this reason lower voltages are also observed in these regions (see Fig. 4).

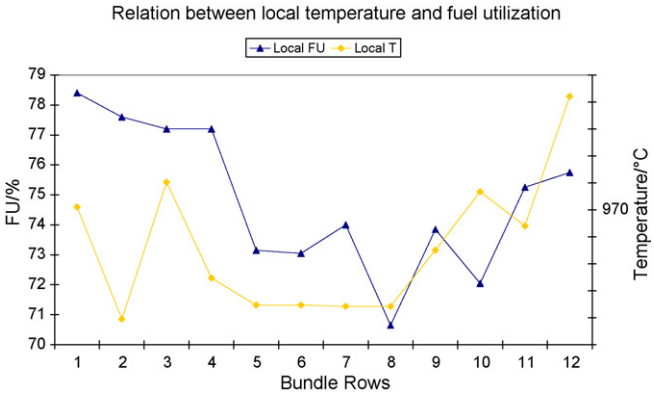

Fig. 17. Distribution of local FU and temperature in the rows of the stack.

In the same Fig. 17 the local temperature distribution is reported. We observe that it seems to exist a relation between the local FU and the local temperature of the rows: the higher is the local FU the higher is the local temperature. Moreover, it could be interesting to consider the fact that the boundary rows (1 and 12) have the reformer unit on the external side characterized by an operation with a reduced amount of fuel gas, compared to the reformation boards placed internally between the inner bundle rows. The amount of the reforming reaction is therefore reduced in these boundary reformers, and therefore its cooling effect is reduced. This could cause the higher values of both local FU and local temperature.

Thus, it is outlined how high local fuel utilization values can lead to local overheating of the generator. Of course, the local overheating causes some problems. First, it limits the operation of the generator, especially the value of current density that the generator can reach, because an increase of current density determines an increase of the local temperature with too high values at the boundary rows. The limitation in the current density means a limitation in the power density of the generator, which is one of the most important parameters of the generator performance. Second, the local overheating can accelerate the degradation of the materials of the tubular cells, causing the degradation of the generator performance and the necessity of a increased maintenance.

To overcome the problem of the local overheating, the first attempt is to analyse the behavior of the system devoted to the thermal regulation of the generator. The thermal regulation is assured by the cathode air flow, which is distributed inside the generator rows. The thermal regulation is made by modifying two factors: the air stoichs and the air pre-heating temperature, but the most important factor is the air stoichs. The air distribution is made with a unique air plenum, which means that the modification of the air stoichs is not differentiate for the different segments of bundle rows, but it is common for the whole generator and the various bundle rows. Therefore, through the use of the sensitivity analysis of the effect of the air stoichs on the local temperature (described in Section 3.2 and shown in Fig. 11), we have determined the sensitivity of the local temperature to a modification of the overall air stoichs factor: the effect is shown in Fig. 18.

The results are shown for the ejectors side, the central zone and the power lead side of the generator. The sensitivity is higher in the central zone (as reported in Fig. 11), but the most important notation is that the sensitivity is almost constant along the 12 bundle rows of the generator, that is, it does not depends on the position of the bundle row inside the generator. Therefore, we can expect that a modification of the air stoichs determines a similar effect in all the bundle rows, that is, the cooling effect is not differentiate in the different zones of the generator. In fact, a modification of the temperature distribution consequent to a regulation of the air stoichs (increase of the air stoichs from

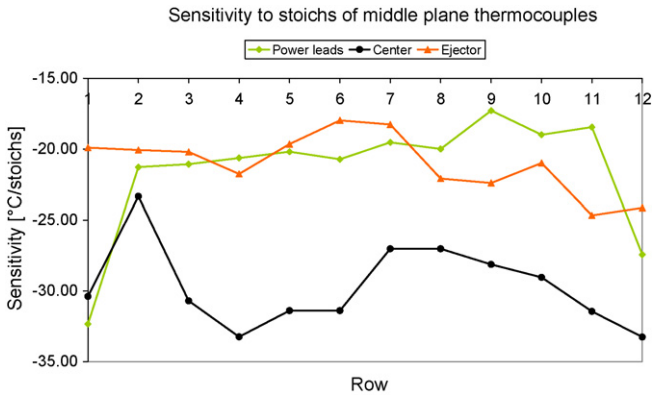

Fig. 18. Sensitivity of the local temperature to a air stoichs regulation.

$\lambda_{air} = 4.6$ to $\lambda_{air} = 4.8$, that is, a cooling of the generator) is shown in Fig. 19 (non-disclosure agreement).

As we see, the thermal regulation through the increase of the air stoichs determines a reduction of local temperature almost uniform along the bundle rows. The regulation does not solve the problem of the local overheating at the boundary rows, and has the consequence of a uniform reduction of temperature, with a decrease of the mean operation temperature of the generator, and a consequent increase of the overvoltages. Therefore, the present air cooling system is able to change the thermal level of the stack, but in a uniform way and cannot act at the local level; therefore it cannot control a local overheating. This limits the possibility of increasing the setpoint temperature, to reduce the overvoltages. But the main drawback is the difficulty of increasing the current density value, with a consequent limitation of the power density of the generator.

An expected thermal regulation of the generator is shown in the figure: a regulation able to obtain an expected uniform value of temperature equal to the setpoint value imposed by the operator. This regulation could be able to overcome the local overheating, while assuring that the mean temperature maintains its imposed setpoint value. This regulation can be obtained through a diversification of the air stoichs imposed in the different zones (or in the different bundle rows) of the generator. The modification has to be made at the level of the air distribution systems, with different air plenums which could differentiate the air stoichs regulation for the different bundle rows.

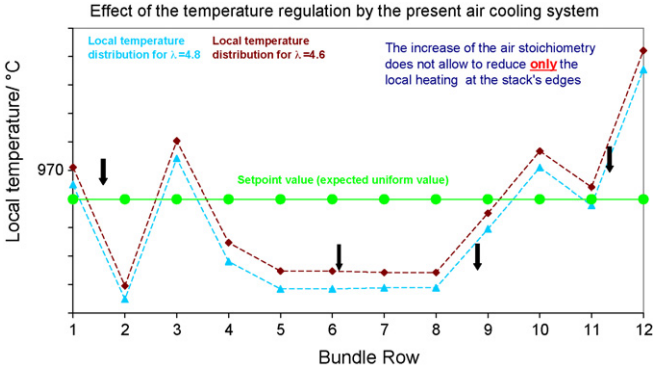

Fig. 19. Effect of the temperature regulation by the present air cooling system.

6. Conclusions

In the paper, an analysis of a SOFC system is presented in terms of sensitivity maps of local voltages and temperatures with respect to the overall fuel consumption and the air stoichiometry control factors:

- the local voltage sensitivity tests to fuel consumption are used as a useful procedure to estimate the local fuel utilization of the main stack's cell sectors during the operation: the local fuel utilization distribution has been found;
- high local fuel utilization have been detected: they can lead to local overheating which can limit the operation (power density, efficiency and degradation) of the generator;
- with the present air cooling system design it is possible to vary uniformly the operating temperature of the generator, but it is not possible to control the local temperature;
- the present air cooling system is able to change the thermal level of the stack, but in a uniform way and cannot act at the local level; therefore it cannot control local heating: this limits the possibility of increasing the current density with a consequent limitation of the power density of the generator;
- a more effective regulation should be able to obtain a uniform value of temperature equal to the setpoint value imposed by the operator; this regulation can be obtained through a diversification of the air stoichs imposed in the different bundle rows of the generator, through the adoption of different air plenums which could differentiate the air stoichs regulation for the different bundle rows.

Acknowledgement

This work was financially supported by Gas Turbine Technologies (Contratto Attuativo 2006), in the frame of the EOS Project.

References

[1] S. Saroglia, P. Leone, M. Santarelli, Eco-efficiency 2005–HYSYDays 1st World Congress of Young Scientists on Hydrogen, Torino, Italy, May 18–20, 2005.
[2] P. Leone, M. Santarelli, M. Calì, J. Power Sources 156 (2006) 400–413.
[3] M. Calì, M.G. Santarelli, P. Leone. Int. J. Hydrogen Energy, in press.
[4] P. Leone, M. Santarelli, Eco-efficiency 2005 – HYSYDays 1st World Congress of Young Scientists on Hydrogen, Torino, Italy, May 18–20, 2005.
[5] M. Calì, M. Santarelli, P. Leone, Comparison of the Behavior of the CHP-100 SOFC Field Unit Fed by Natural gas or Hydrogen through a Computer Experimental Analysis, World Hydrogen Technology Convention, Singapore, 2005.
[6] M. Calì, E. Fontana, V. Giaretto, G. Orsello, M. Santarelli, HySafe—International Conference on Hydrogen Safety, Pisa, Italy, 2005.
[7] D.C. Montgomery, Design and Analysis of Experiments, John Wiley & Sons, Inc., 2005.
[8] R.E. Walpole, R.H. Myers, Probability and Statistics for Engineers and Scientists, Prentice Hall International Inc., New Jersey, 1993.
[9] M. Cali, F. Debenedictis, P. Leone, M. Santarelli, V. Verda, ASME 1st European Fuel Cell Technology and Applications Conference, Rome, Italy, December, 2005.
[10] M. Calì, P. Leone, M. Santarelli, G. Orsello, G. Disegna, General Topics and Operation Description by Means of Regression Models,

World Hydrogen Energy Conference WHEC 2006, Lyon, France, June, 2006.
[11] M. Calì, G. Orsello, M. Santarelli, P. Leone, Proceedings of ESDA2006, 8th Biennial ASME Conference on Engineering Systems Design and Analysis, Torino, Italy, July, 2006.
[12] M. Santarelli, P. Leone, M. Calì, F. De Benedictis, Lucerne Fuel Cell Forum 2006, Lucerne, Switzerland, July, 2006.
[13] S. Gopalan, G. DiGiuseppe, J. Power Sources 125 (2004) 183–188.
[14] M. Molinelli, D. Larrain, N. Autissier, R. Ihringer, J. Sfeir, N. Badel, O. Bucheli, J. Van Herle, J. Power Sources 154 (2006) 394–403.
[15] R.A. George, J. Power Sources 73 (1998) 251–256.
[16] S.C. Singhal, K. Kendall, High Temperature Solid Oxide Fuel Cells: Fundamentals, Design and Applications, Elsevier, 2004.
[17] H. Kabs, Operational Experience with Siemens-Westinghouse SOFC Cogeneration Systems, Lucerne Fuel Cell Forum, 2001.
[18] M. Santarelli, P. Leone, M. Gariglio, M. Calì, P. Spinelli, G. Orsello, F. De Benedictis, Fuel Cell Seminar 2006, Honolulu, Hawaii, USA, 2006.
[19] S.C. Singhal, in: W. Poulsen, N. Bonanos, S. Linderoth, M. Mogensen, et al. (Eds.), Proceedings of the 17th Riso International Symposium on Materials Science: High Temperature Electrochemistry: Ceramics and Metals, Riso National Laboratory, Roskilde, Denmark, 1996, p. 123.
[20] K.S Huang, Cell Power Enhancement via Materials Selection, 7th European SOFC Forum, Lucerne, Switzerland, July 3–7, 2006.
[21] S.D. Vora, Advances in Solid Oxide Fuel Cell Technology (SOFC) at Siemens Westinghouse, Fuel Cell Seminar, Palm Springs, California, USA, November 14–18, 2005.
[22] R. Draper, G. DiGiuseppe, Proceedings of ASME European Fuel Cell Conference, Rome, Italy, December 14–16, 2005.
[23] J. Kim, A.V. Virkar, K.Z. Fung, K. Metha, S.C. Singhal, J. Electrochem. Soc. 146 (1) (1999) 69–78.